STATISTICAL PROPERTIES OF

SPECTRA

By C. E. Porter

THE purpose of this paper is to present a rapid survey of the statistical properties of spectra, using both atomic spectral data and nuclear spectral data. In many cases, only one kind of relevant data exists; for example, very little is known about atomic-particle transition-probability data, so in such areas we must confine our attention to nuclear data. When both atomic and nuclear data are available, we have tried to select those data which are usually not treated according to the general approach of this paper. Throughout our discussion, then, we will be mainly emphasizing analogies and the manner of handling different sorts of data according to the spirit of this paper.

Spectra

What are energy spectra? In this discussion we shall always have in mind the energy spectra of a many-nucleon nucleus or a many-electron atom (or molecule), both of which are outstanding examples of complex many-particle systems for which a statistical treatment is appropriate. In order to understand what is meant by energy spectra, it is convenient to develop our discussion by comparison with the more familiar many-planet solar system. In the case of the planetary system the planets play a role similar to the electrons in a complex atom with the sun at the center taking the part of the nucleus. Similarly it is now fashionable to think of the nucleons in a nucleus as though they move in a central field which could be compared to the gravitational field of the sun, making the solar system analogy good in a qualitative sense for both the atom and the nucleus. In the nuclear case, the attractive central field in which the nucleons move is created completely by the nucleons themselves, so that the fields created by the nucleons enter into the nuclear system in a more complex way than is usually imagined as a firstapproximation picture of the solar system or of a many-electron atom, but we shall ignore this complication for the present.

There are two kinds of orbits in the solar system, those of the planets, which are bound orbits, and of (noncyclic) comets, which traverse the solar system in unbound orbits. A comet can thus be said to be an unbound planet. These different orbits have different total energies, and the different energy states constitute the energy spectrum of the solar system. The planetary spectrum is sketched in Fig. 1.

The energy spectrum of the solar system is continuous (note the shading in Fig. 1) and runs from an energy of negative infinity for tightly bound (planetary) orbits through zero energy making the

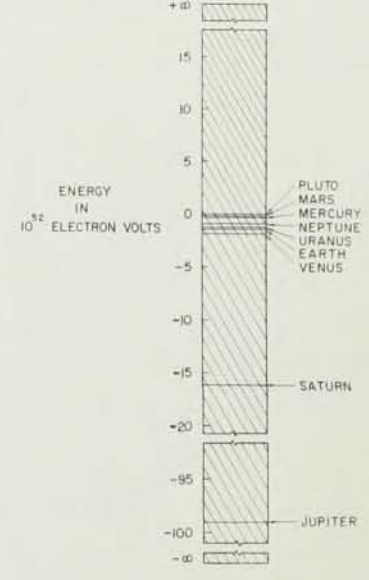


Fig. 1. Spectrum of solar system. Note the broken energy scale. Shading emphasizes the continuous character of the spectrum.

Charles E. Porter, a physicist at the Brookhaven National Laboratory, presented the paper on which this article is based as an invited address before the American Physical Society on April 25, 1962,

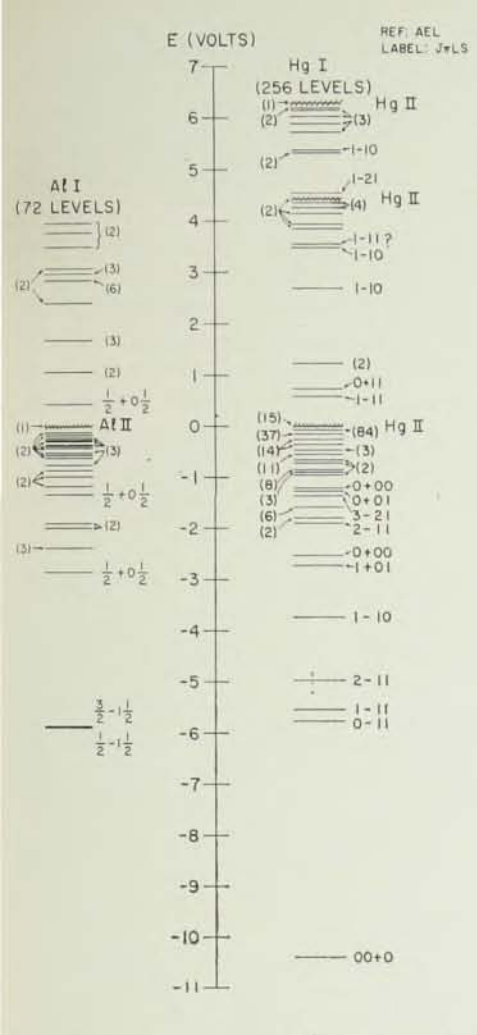


Fig. 2. Atomic energy levels of neutral aluminum (AlI) and neutral mercury (HgI) taken from reference 15. Numbers not in parentheses labeling the levels are $J\pi LS$, and the numbers in parentheses indicate a cluster of that number of levels lying too close together to be drawn separately. Note especially the large number of discrete unbound levels.

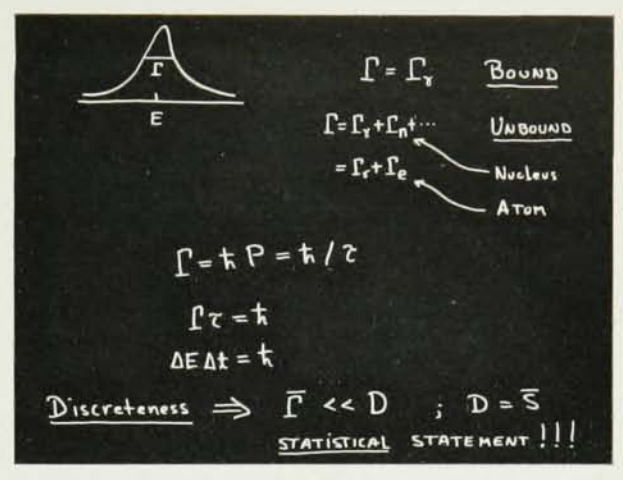


Fig. 3. Summary of the characterization of a discrete energy state. The total width of a nuclear level includes the total radiation width, the neutron width, etc., while that for an atomic level includes a total radiation width and an electron width. The usual energy-time uncertainty connection between width and lifetime holds, of course.

transition to unbound (comet) orbits which may have energies up to positive infinity (in principle) as is indicated in Fig. 1. It should also be pointed out that an unbound orbit can be thought of as a scattering orbit; i.e., the comet is scattered by the solar system.

For a wave-mechanical system (which the atomic and nuclear systems are) only non-self-destructive wave phenomena are allowed. This additional requirement upsets the continuous character of the spectrum, changing a typical energy spectrum into a partly discrete, partly continuous spectrum. In a more accurate sense, the spectrum remains continuous but is modulated into more dense and less dense countable (hence discrete) groups. Crudely speaking, if a wave is not to be self-destructive, an integral number of wavelengths must fit into the orbit of the particle, and this is how the element of countability or discreteness is introduced into the spectrum. The spectra of two typical atoms, neutral aluminum (AII) and neutral mercury (HgI), are shown in Fig. 2

First of all, we see that there is a ground state for

the system at $-E_0$ which is bound by the finite energy E_0 . Thus no infinitely tightly bound orbits are allowed in the wave-mechanical system. Near the ground state, the spacing between the discrete levels is typically rather large and decreases rapidly as the unbound states are approached. The unbound discrete states are (in the nuclear spectrum at any rate) very closely spaced, and they eventually overlap and merge into an unresolvable continuum.

Of all of the states indicated in Fig. 2, only the ground state $-E_0$ can be completely stable. (We shall ignore beta-decay effects in this article.) All of the excited (nonground) bound states are unstable with respect to radiative decay (emission of light), and the unbound excited states are unstable with respect to the emission of particles (electrons in the atom or nucleons or nucleon clusters in the nucleus) as well as light emission. (By definition any unbound particle can run away like a comet.)

Each of the excited states has an intensity profile similar to that sketched in Fig. 3. The total width Γ of the state is indicated as well as the energy position E of the state. Also pointed out in the figure are the

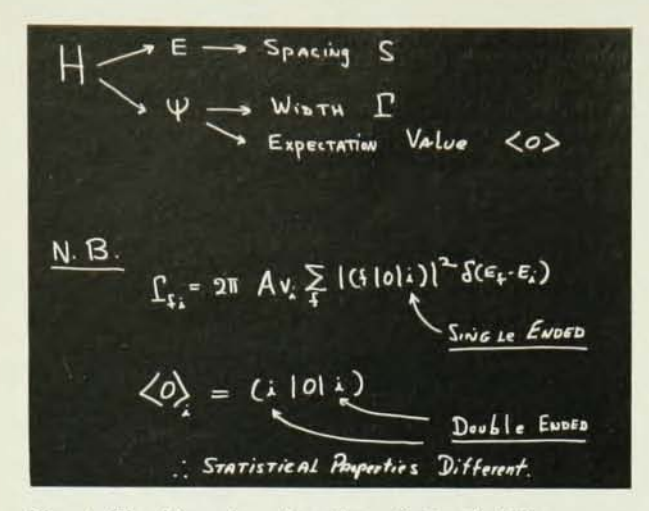


Fig. 4. The hierarchy of a theoretical calculation is indicated with the Hamiltonian of the system as a starting point. It is important to note that spacings, widths, and expectation values all follow from hypotheses with respect to H. The major statistical difference between the "single-ended" character of a width and the "double-ended" character of an expectation value is also indicated.

connections between width Γ , transition probability P, and mean life τ and the usual time-energy uncertainty relation. It is emphasized in the figure that the discreteness of a spectrum is a statistical property, since the mean width must be much less than the mean spacing between states in order that they be countable.

It is perhaps worth stressing that models of spectra are almost always stable (e.g., even the usual models of the hydrogen atom). This is a property only of models and not of real spectra.

We now sketch briefly the theoretical source of the properties of spectra. In Fig. 4 the usual connections are indicated. The energies E and the wave functions ψ of the states come from the Hamiltonian H of the system via the Schrödinger equation. These in turn give the energy-level spacings S, the level widths Γ , and expectation values <O> of a relevant operator O. It is emphasized in the figure that the statistical properties of the widths and expectation values differ because of the off-diagonal and diagonal character of the matrix elements involved.

The concept of degeneracy is very important for us. We must now take notice of the additional labels on the energy levels in Fig. 2. These labels are associated with symmetry properties of the Hamiltonian H of the system. As indicated in Fig. 5, typical labels are the total angular momentum J, the parity π , the total orbital angular momentum L, the total spin angular momentum S, the energy E, and the possibility of making the matrix elements of the

Hamiltonian H real. Each of these additional constants of the motion is associated with a symmetry transformation as shown in the figure. In particular, the reality of the matrix elements of H is a consequence of the assumed time reversal invariance of the Hamiltonian.

Two levels which coincide in energy are said to be degenerate. The general feature of degeneracy is that energy levels with the same symmetry labels do not in general coincide, i.e., are not degenerate. Thus, it is said that levels of the same symmetry "repel" each other. Another way to say this is that the nearest-neighbor spacing between two levels of the same symmetry does not vanish. We will discuss statistical degeneracy later in terms of energy-level spacing statistics.

Average Properties of Spectra

The average properties of spectra are much more complicated to present than the fluctuations. The reason for this is that the fluctuation laws are independent to a good approximation of the specific system (and hence the specific forces being considered) much in the same way that the well-known Gaussian distribution arises in many different connections in practice. (The physical significance of the average values may be quite different, even though the fluctuation law is the same.)

The basic average property is the mean level density. A very complete review article on this subject has been written by Torleif Ericson. We content ourselves here with a typical plot of some atomic energy-level data (Ericson discusses only nuclear data when he refers to experiments) to indicate how such data are usually handled. In Fig. 6 are plotted

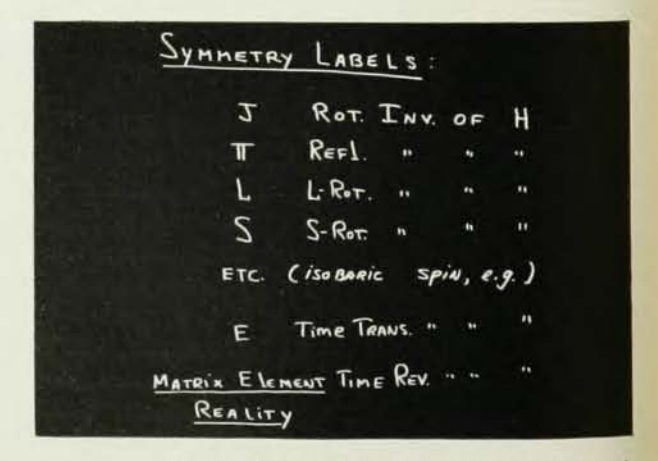


Fig. 5. A list of typical symmetry labels is given. For later reference, we emphasize the association between matrix-element reality and time-reversal invariance.

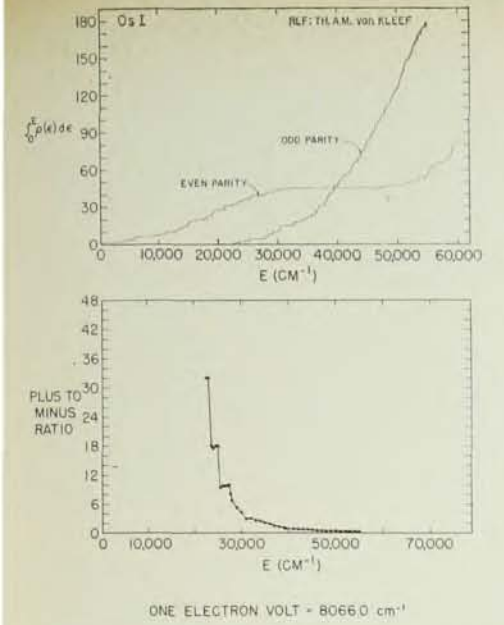


Fig. 6. Upper part of figure shows cumulative energy-level distribution data⁸ for even and odd parity states of neutral osmium (OsI). Probably missing are even parity levels in the 30 000 to 50 000 cm⁻¹ range. Lower part of figure shows ratio of two upper curves, giving a typical average parity statistic when smoothed. Note that there are parity fluctuations at low excitation. Complete theories of these effects are lacking.

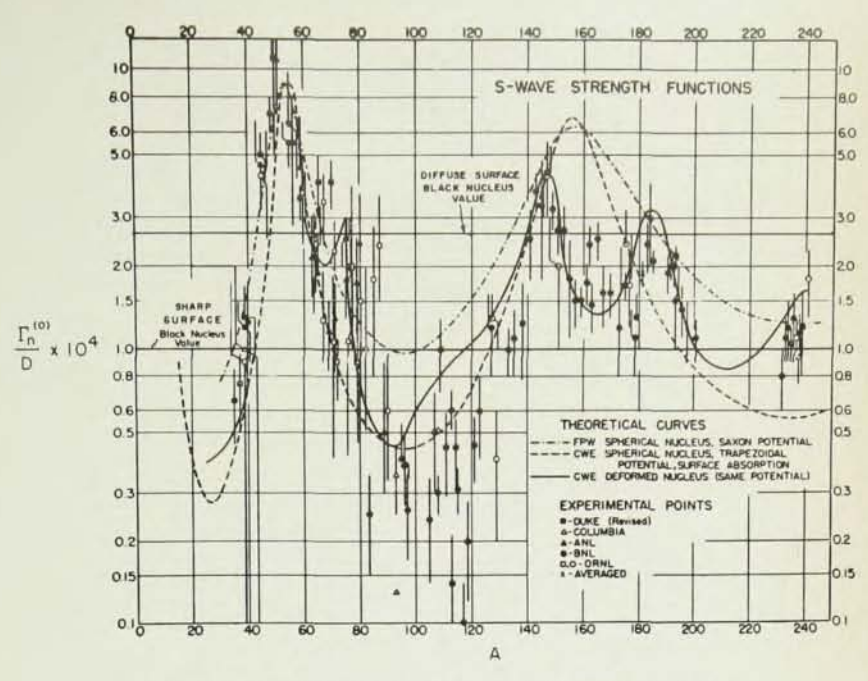


Fig. 7. Experimental (points) and theoretical (curves) S-wave strength functions (conductive property of spectra). The theoretical computations are explained in the text. (Figure made available to the writer by J. A. Harvey.)

in the top part of the figure the cumulative number of levels,

$$\int_{0}^{E} \rho(\epsilon) d\epsilon,$$

as a function of excitation energy E for neutral atomic osmium (OsI) as obtained by van Kleef.² As each new level appears, a unit vertical step is taken in the histogram. Note that the levels have been separated according to parity and that there is a definite indication that a number of even parity levels have been missed between 30 000 and 50 000 cm⁻¹. (The probable missing of levels was pointed out to the writer by R. E. Trees.) The steep rise of the odd-parity level density resembles the typical exponential rise of theoretical level densities. Of course, the actual level density is the slope of the curve.

In the lower part of Fig. 6 is plotted the ratio of the total number of positive parity levels to the total number of negative parity levels. There are noticeable fluctuations in the plot (which we will not discuss in this article), but the ratio eventually settles down to a number close to one.

For the moment, we omit discussion of average expectation values (we will come to gyromagnetic ratios when we discuss fluctuations) and turn our attention to average quantities associated with instability. The first of these is the strength function (a

conductive property of spectra), which can be defined for any type of channel (electron, gamma ray, fission, etc.), but which has mainly been measured for neutrons incident on nuclei. (It would be very interesting to know the electron strength function of neutral or ionized atoms.) In Fig. 7 we show the current data along with theoretical calculations for S-wave neutrons. The label FPW (Campbell, Feshbach, Porter, and Weisskopf³) stands for a potential of the Eckart form with

 $R = 1.15 A^{1/3} + 0.4 \text{ fermi,}$

V = 52 MeV,

W = 3 MeV,

d = 0.52 fermi,

while the initials CWE (Chase, Wilets, and Edmonds⁴) stand for the parameters (with a trapezoidal potential)

 $R = 1.35 A^{1/3}$ fermi,

V = 44 MeV,

W = 2.2 MeV,

 $\Delta = 2.2 \text{ fermi} = 90\% - 10\% \text{ distance},$

 β = distortion taken from E2 transition data (variable from nucleus to nucleus).

Note that the black nucleus value for diffuse surface potentials differs from that for sharp surface

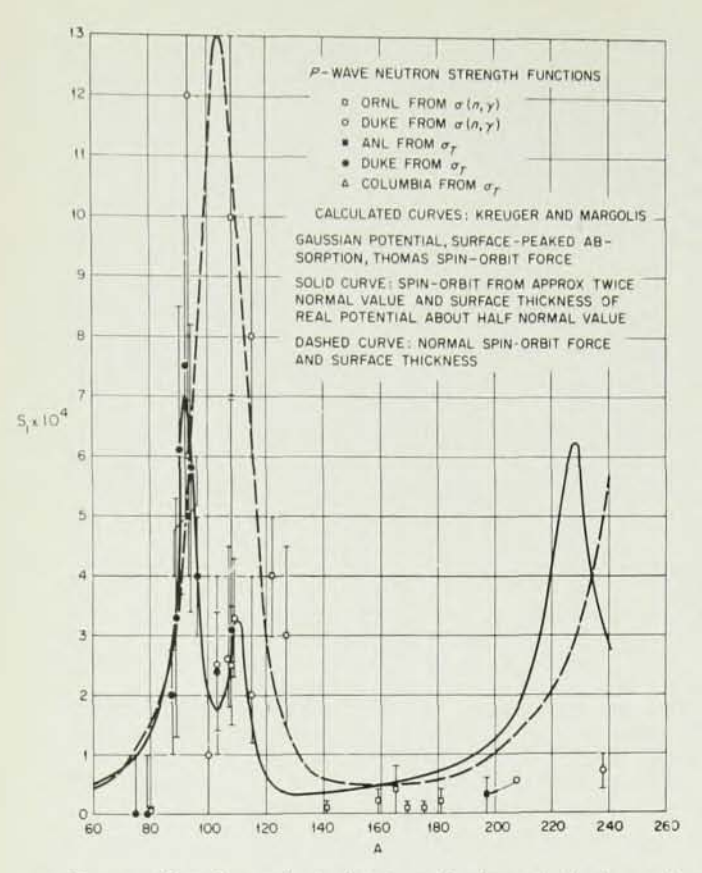


Fig. 8. Experimental (points) and theoretical (curves) P-wave strength functions. (Figure courtesy J. A. Harvey).

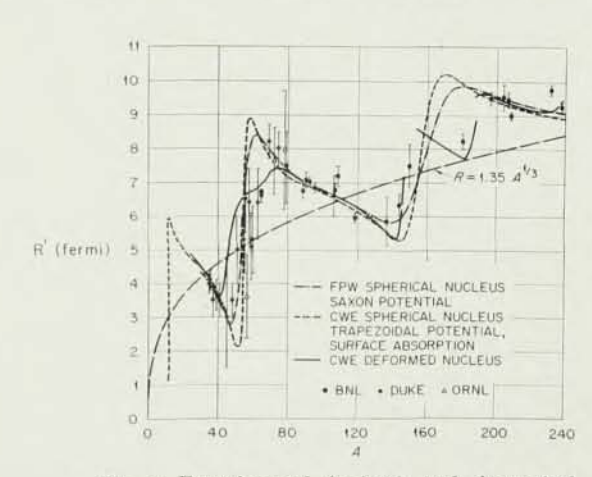
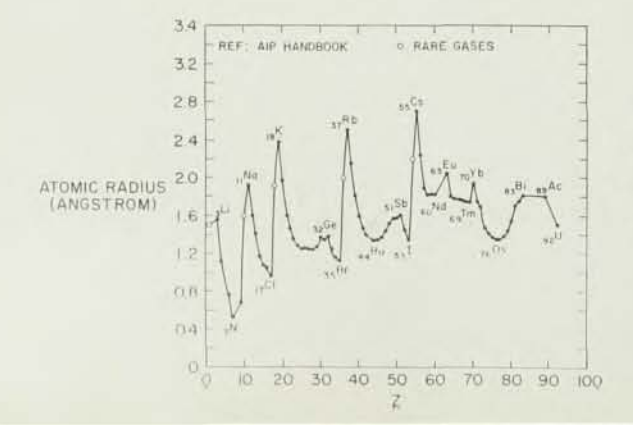


Fig. 9. Experimental (points) and theoretical (curves) S-wave potential scattering amplitude (susceptive property of spectra). The theoretical computations correspond to those in Fig. 7.



potentials. Fig. 8 shows similar results for the P-wave strength function at low energies. The calculated curves are taken from Kreuger and Margolis. The parameters used differ from the usual sets, especially since they find a need for a rather large spinorbit coupling. Recently, relevant computations of strength functions have been made by Perey and Buck using a nonlocal optical potential. These authors are able to achieve an unusually good interpolation through the experimental data with no explicit energy dependence in their parameters.

The other type of quantity associated with instability is the susceptive property or "potential" scattering length R'. Data and numerical computation of this quantity are shown in Fig. 9. The references in the figure follow the same pattern as those in Fig. 7.

In Fig. 10 are plotted atomic radii as taken from the American Institute of Physics Handbook. In a sense, these radii represent a susceptive property of atoms. There are a few notable features in this plot. First of all, the over-all trend of the radius is an increase, not a variation of Z^{-1/3} as predicted by the Thomas-Fermi model of the atom. Secondly, the rare gases have unusually large radii. Unfortunately, the AIP Handbook does not describe the experiments on which these radii are based. In any event, there seems to be every motivation for further measurements of radii by electron scattering from atoms to see if such radii are compatible with those plotted in the figure.

Fluctuations

Since we opened our discussion of the average properties of spectra with the density of energy levels, it is natural to begin the discussion of fluctuations with comments on the distribution of energy-level spacings. (We repeat here that the fluctuation laws are not system (or force) dependent in the way the average quantities are, so that the laws are in this sense more universal.) We recall that statements about energy-level spacings are natural ways to comment about the degeneracy of the spectrum. We expect that if we include levels with many, many different symmetry labels (spin and parity) in our sample, then we are confronted with an ordered (in energy) sequence of random numbers. Let $x = S/\bar{S} = S/D$, where S is the nearest-neighbor spacing and

Fig. 10. Plot of atomic radii taken from American Institute of Physics Handbook versus atomic number. In a sense this is a susceptive property of atoms. Note the gradual increase of the radius as opposed to the Thomas-Fermi $Z^{-1/3}$ law. Also, the rare gases have very large radii.

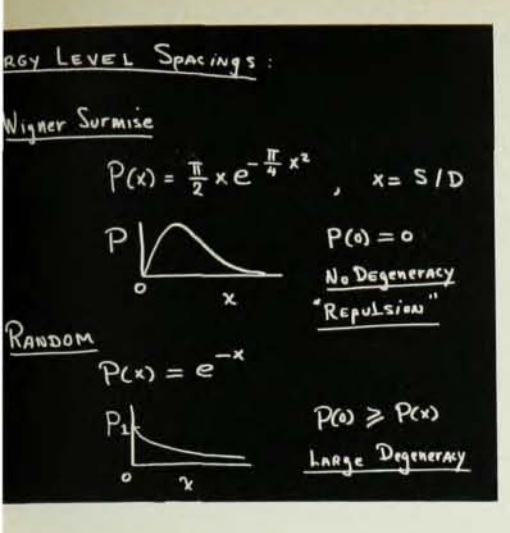
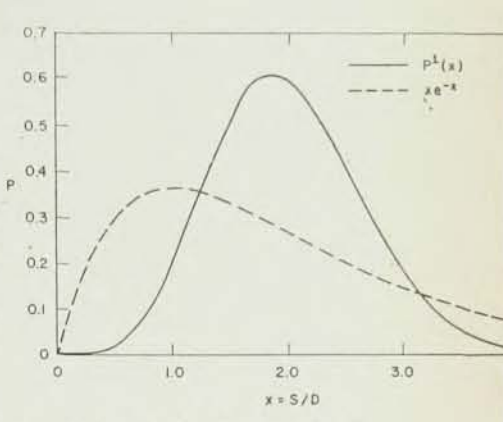


Fig. 11. Summary of simple nearest-neighbor spacing theory. The contrast between nondegenerate and the highly degenerate cases is to be noted. Wigner's surmise can be obtained either from the argument in the text or from the two hypotheses of rotational form invariance and independence for 2 × 2 matrices.

Fig. 12. Plot of the next-nearest-neighbor spacing distribution $P^1(x)$ as a function of x and also the Poisson next-nearest-neighbor spacing distribution $x \exp(-x)$. The large repulsion effect near x = 0 is very much in evidence.



D is the mean distance between levels. Then, if f(x)dx is the probability that, given a level at x=0, there is a level in dx at x, it is possible to show that $\exp[-f_0^x f(t)dt]$ is the probability that the interval (0,x) is empty of levels; so we have for the spacing probability distribution:

$$P(x)dx = \exp\left[-\int_0^x f(t)dt\right]f(x)dx, \qquad (1)$$

where we have multiplied (infinitesimally) the probabilities that dx contain a level and that the interval (0, x) be empty. Equation (1) implies:

$$P(x) = f(x) \exp\left[-\int_0^x f(t)dt\right]. \tag{2}$$

If f(x) = const., then the (properly normalized) result for P(x) is:

$$P(x) = \exp(-x), \tag{3}$$

which is the familiar Poisson distribution for the nearest-neighbor spacing between an ordered sequence of random numbers. Perturbation theory for real symmetric matrices indicates that f(x) is linear in x for small x. If we assume this to be generally true, letting $f(x) = (\pi/2)x$, we find:

$$P(x) = (\pi/2)x \exp \left[-(\pi/4)x^2\right]. \tag{4}$$

This is the famous surmise of Wigner. These results are summarized in Fig. 11. Incidentally, (4) also follows from the hypotheses of rotational invariance and independence for 2×2 matrices and is in surprisingly good agreement, as shown by explicit Monte-Carlo machine computations and by the ana-

lytical methods of Gaudin and Mehta, with the theoretical nearest-neighbor spacing distribution for very large matrices.

We show in Fig. 12 the next-nearest-neighbor spacing distribution $P^1(x)$ and the corresponding Poisson distribution $x \exp(-x)$. The former of these is derived from the two hypotheses of rotational invariance and independence for 3×3 matrices.

In Fig. 13 we show nuclear level spacing data⁷ for states of spin $\frac{1}{2}$ and even parity (Th²³², U²³⁴, U²³⁶, U²³⁸ targets with neutrons incident) in the left-hand part of the figure. The solid curve is (4).

Next we come to the fluctuations of quantities associated with instability, viz. the partial level widths. The simplest of such quantities is a particle width of an autoionizing level. Since there is no atomic data on autoionizing widths available, we show, on the right-hand side of Fig. 13, nuclear neutron-width data.⁷ The solid curve is half of a simple Gaussian:

$$P(y) = (2/\pi)^{1/2} \exp(-y^2/2),$$
 (5)

which is a consequence of the assumption of rotational invariance (representation independence) of the theory. To derive this we recall that a width for level λ and channel c is given in terms of a reduced width amplitude $y_{\lambda c}$ as

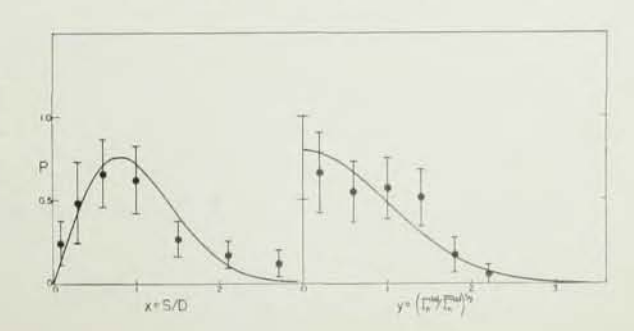
$$\Gamma_{\lambda c} = 2P_e y_{\lambda c}^2, \tag{6}$$

where

$$y_{\lambda e} \propto \int X_{\lambda} \Phi_e dS.$$
 (7)

Here, X_{λ} is the level function, Φ_c is the channel function, and the integral is (3A-1)-dimensional with

Fig. 13. Plots of experimental (points) and theoretical (curves) spacing and neutron-width distribution data. Agreement is seen to be quite good.



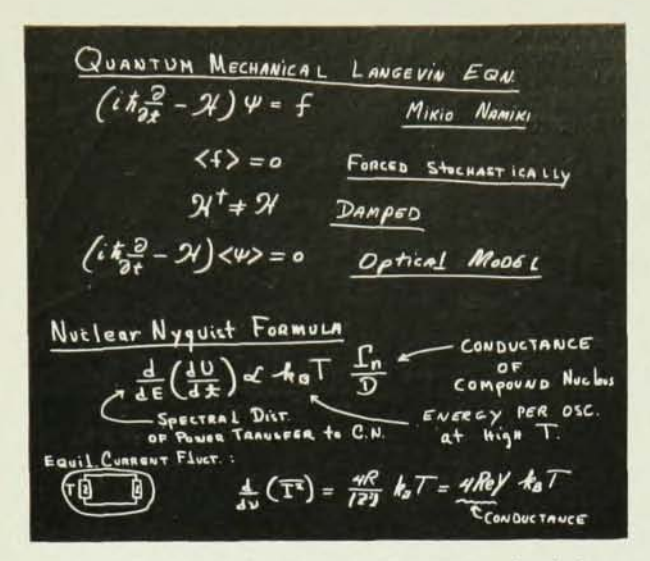


Fig. 14. Summary of the quantum-mechanical Langevin equation of M. Namiki and the resulting Nyquist formula, a fluctuation-dissipation theorem. Optical model, when used for very light elements ¹⁶ represents dissipation without fluctuation.

A the number of particles in the compound system. Picking an orthonormal "coordinate system" ψ_{μ} , we can expand X_{λ} to give

$$y_{\lambda c} \propto \sum_{\mu} a_{\lambda \mu} \int \psi_{\mu} \Phi_{c} dS,$$
 (8)

in which the $a_{\lambda\mu}$ are the components of X_{λ} . Rotational invariance means the a's are equally likely to be positive or negative and are, for a vector space of high enough dimension, most likely to be zero. Thus (8) expresses the net displacement in a one-dimensional random walk, giving immediately a Gaussian distribution for $y_{\lambda c}$, or equivalently (5), in which y is scaled such that $\langle y^2 \rangle_{av} = 1$.

It is of course an immediate step to ask about other widths. The nuclear total-fission width behaves in a rather singular manner, since there is a collectivedistortion-intermediate-state correlation among the partial-fission widths. In contrast to an anticipated multichannel behavior, the total-fission width fluctuates almost like a neutron width. Not much information is yet available on the partial-fission widths associated with individual fragment pairs.

Both total and partial nuclear radiation widths have been measured. The total radiation width is found to be almost constant. On the other hand, the partial radiation widths⁸ fluctuate as though the radiative matrix element were a complex number (two degrees of freedom). From time-reversal invariance arguments (Lloyd Theorem) it is known that the matrix element must be real (as must a beta-decay matrix element), so that some sort of special structure in the partial widths is indicated.

Very little highly accurate atomic or molecular radiation-width data is available at present. A preliminary examination of a recent compilation¹⁸ of atomic radiation-width (transition = probability) data indicates widely fluctuating widths. There is every reason to make more accurate measurements of these quantities, as well as of electron widths for autoionizing states about which next to nothing is known experimentally.

We now digress a moment to point out the connection between the neutron-width distribution and the more familiar notions of Johnson noise in an electrical system. It has been shown by Namiki⁹ that it is possible to write a Langevin type of equation for the Schrödinger equation. Such an equation is a damped, stochastically forced wave equation. As a consequence of this equation, a nuclear (or atomic) Nyquist formula is obtained relating the spectrum of the power transfer to the strength function. These results are summarized in Fig. 14.

In Fig. 15 we show, among other things, the imaginary part of the optical potential computed for atomic argon¹⁰ (electrons incident on neutral argon).

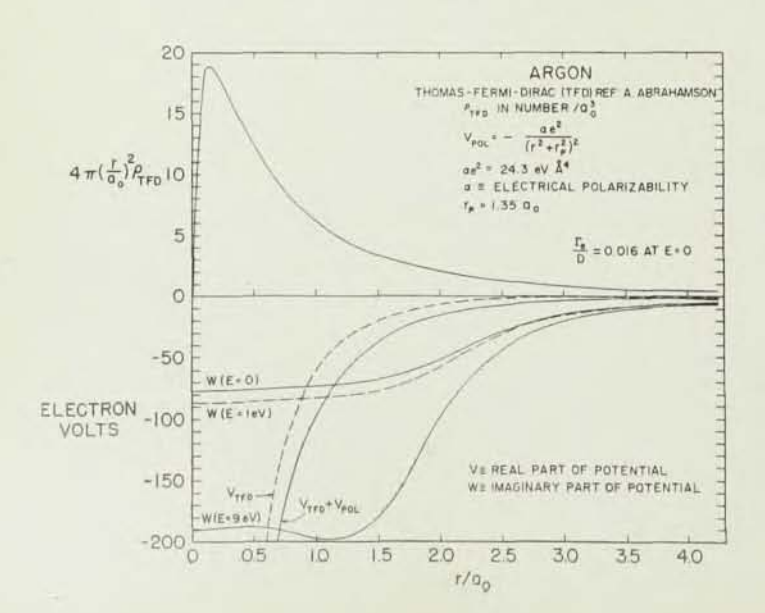
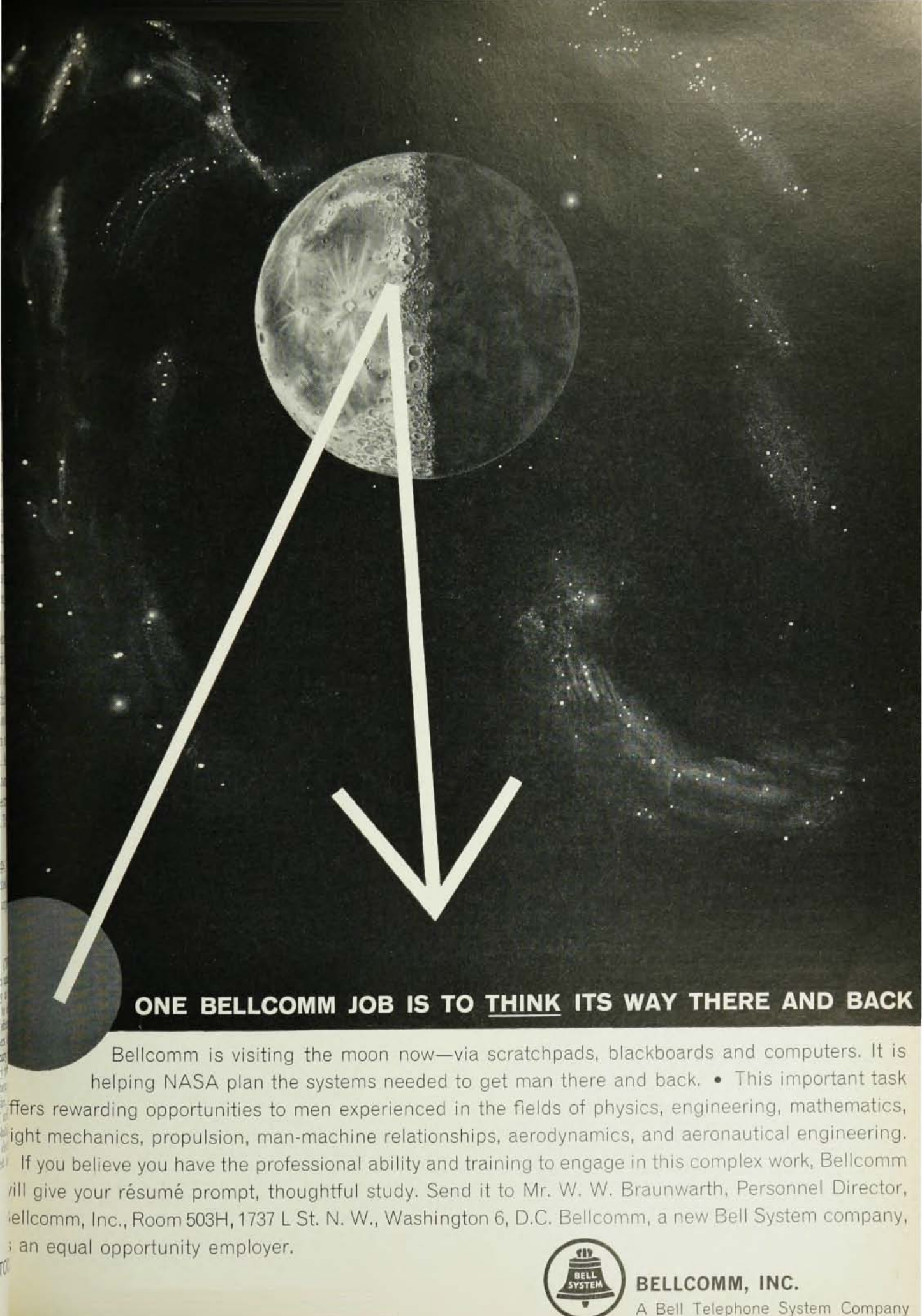


Fig. 15. Plots of Thomas-Fermi-Dirac (TFD) potential and density 17 for neutral argon against r/a_0 . Density has been cut off smoothly at the S-wave hydrogenic value Z^3/π at r=0 to eliminate the usual $r^{-3/2}$ singularity. This effect is hardly noticeable on the plot but enters in a critical way into calculation of the imaginary part of the potential. The calculated imaginary part is shown for various values of electron energy assuming a screening radius of atomic size. This assumption appears wrong, and both W and the electron strength function Γ_e/D are probably an order of magnitude or two too large. An electrical polarizability must of course be included in the real part of the potential as indicated.



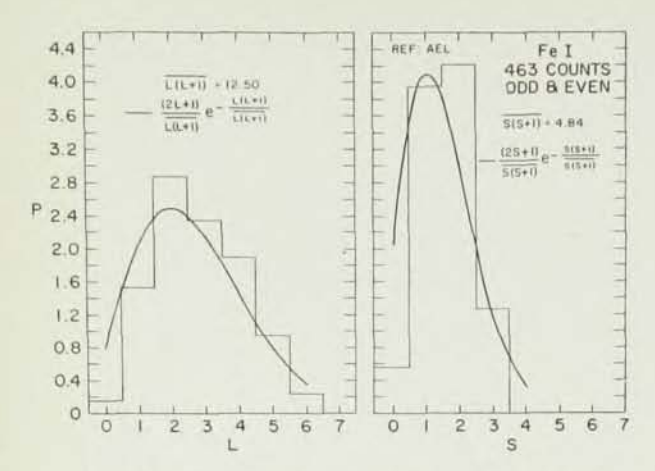


Fig. 16. Plots of the orbital and spin angular-momentum distributions for neutral iron (FeI) ¹⁵. Solid curves are the usual theoretical curves; the single average ("moment of inertia") parameter is indicated in the graphs.

The imaginary part is most likely overestimated by one or two orders of magnitude since it will probably not be compatible with the Ramsauer scattering data. This indicates a probable overestimation of the screened electron-electron cross section. Clearly, further experiments are to be desired. Also extensions of computations of W to atom-atom, atom-molecule, and molecule-molecule scattering may prove to be useful.

We have not yet mentioned correlations which may exist. Present theories predict no correlation between the eigenvalues and the eigenvector components so that any correlation between spacings and widths or spacings and expectation values (e.g., the gyromagnetic ratios which we shall come to shortly) are predicted to vanish. On the other hand, nonzero spacing-spacing correlations and, at least in principle, width-width correlations are predicted. The adjacent nearest-neighbor spacing correlation coefficient is predicted to be about -25% and the width correlation coefficient is of the order of the negative of the reciprocal of the dimension of the vector space involved. This reciprocal is usually small, since the dimension of the vector space under consideration is usually large.

The status of the experimental evidence concerning correlations is mixed. The width-width correlations seem to be small (less than 10%) while the spacing-spacing correlations are in rough correspondence with the predicted anticorrelation. So far, the width-spacing correlation found in the data is small. This is consistent with the invariance hypothesis.

Atomic energy-level data are very convenient for the study of angular-momentum distributions. In Fig. 16 are shown the experimental results for neutral iron (FeI). We have not discussed theories¹¹ of the average parameters in these distributions since no complete theories exist, but the data indicate the order of magnitude of the results that can be expected. The solid curves in the figure are simple theoretically motivated (from some kind of rotator) functions as indicated. Mainly, we view the angular-momentum distribution as a preliminary to the gyromagnetic ratio distribution, and since *LS* coupling is good for FeI, that atom affords an opportunity to study the angular-momentum distribution.

The gyromagnetic ratio is an example of an expectation value or of a "double-ended" quantity in the sense of Fig. 4. The relevant equations are summarized in Fig. 17. We see at once that the Landé g depends explicitly on L and S and that, for a complex atom in which L and S are not good quantum numbers, a connection exists between g_{α} (in the representation α) and the Landé g. The relevant direction cosine (eigenvector component) is the same sort of component that enters into the partial widths in (8), but, because of the double-ended character of an expectation value, the structure of the equations is different.

The first few moments of g are shown also in Fig. 17 in their connection to the moments of the Landé g's. For high dimension, the dispersion of the actual g's is reduced from that of the Landé g's by a factor $\left[\frac{2}{N+2}\right]$ if the state specified by the label α is a random mixture of LS states.

In Fig. 18 is shown experimental data on the gyromagnetic ratios of the states of neutral osmium (OsI).

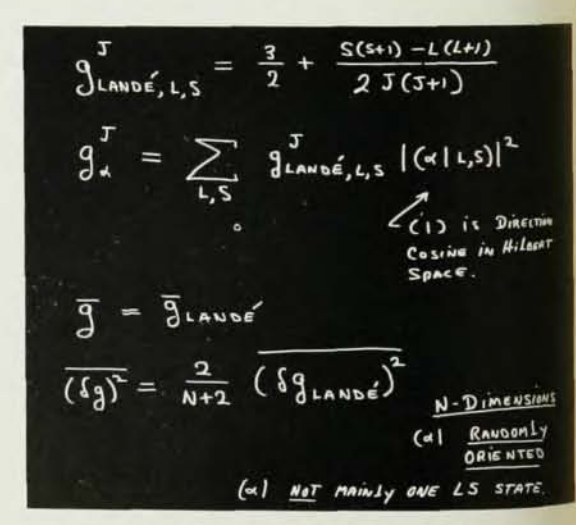


Fig. 17. Summary of the gyromagnetic ratio equations. The Landé value is given along with its connection to an arbitrary representation labelled by α . Especially the dimensional "damping" factor 2/(N/2) in the gyromagnetic ratio dispersion for randomly oriented α is very important.

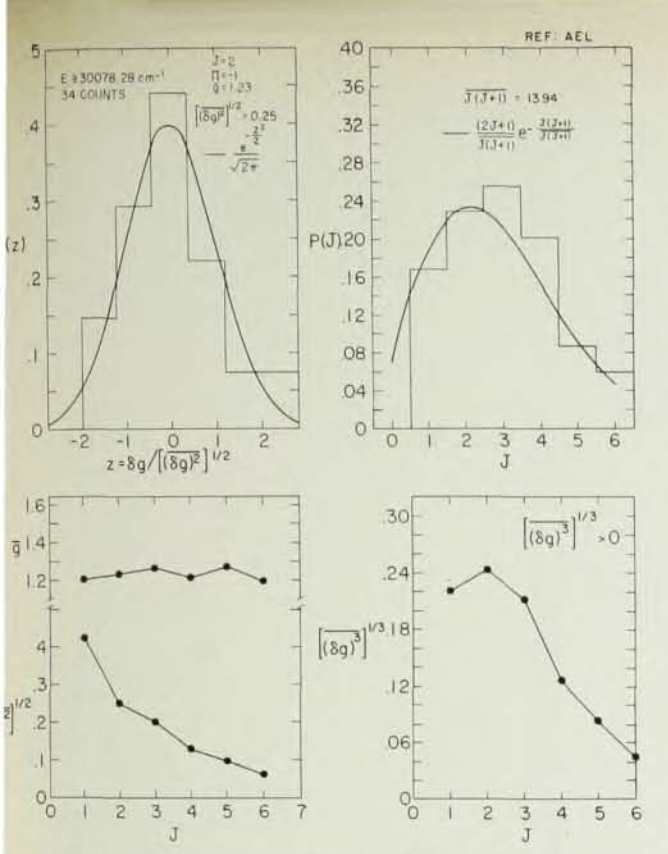


Fig. 18. Gyromagnetic ratio data ¹⁵ for neutral atomic osmium (OsI). A plot of the gyromagnetic ratio distribution for spin-two odd-parity states is shown along with a Gaussian curve. The total angular momentum distribution in osmium is also shown. In addition, the first few moments of the gyromagnetic ratio distributions for different total spin are plotted against total spin. There is a significant third (odd) moment so that the Gaussian is only roughly correct as a limiting distribution.

Neutral osmium has a complex spectrum in which L and S are not good quantum numbers. The figure shows the g-distribution for states of odd parity and a spin of two. In addition, the total angular-momentum distribution, as well as the first three moments of the g-distribution as a function of angular momentum, are shown. The decrease of the second and third moments with increasing angular momentum is evident. This can be ascribed to the dependence on J in the Landé g-value.

We close our discussion with a few remarks on the theoretical models for the fluctuations. Recalling from Fig. 5 that time-reversal invariance implies real matrix elements for the Hamiltonian H, we restrict our attention to theories which are invariant against orthogonal (real unitary) transformations in a vector space of dimension N. If we also add the requirement that the matrix elements of H be independently dis-

tributed, then there is an "if-and-only-if" theorem based on the hypotheses of invariance and independence which concludes that the distribution of H must be of the form indicated in Fig. 19. From this distribution all of the consequences we have mentioned for the eigenvalues (spacings of levels with the same symmetry) and eigenvector components follow in principle according to the hierarchy in Fig. 4.

In practice, extracting mathematical results has proved to be very difficult when at all possible. The work12 of Mehta and Gaudin as well as the complex mathematical problems encountered by Dyson¹³ in his work on circular ensembles show the nature of the difficulties. Rosenzweig14 has shown how to meet Dyson's objection to the nonuniform weighting of the Gaussian ensemble summarized in Fig. 19 by proposing a slightly different ensemble which becomes asymptotically identical to the Gaussian ensemble as the dimension N of the vector space is increased. In addition, many (not all-the single eigenvalue distributions are different) of the asymptotic (large N) results for the circular ensemble of Dyson are identical to those of the Gaussian ensemble, so that there is in practice little distinction among the mathematically solvable models, except in the way in which the circular ensemble must ignore the width and expectation value problem.

This latter problem of quantities derived from eigenvectors is an important one, and therefore acts in strong support of theories which induce a measure directly on the (non-group-forming) Hamiltonian matrices, with a consequent built-in prediction for the eigenvectors as well as the eigenvalues. Since

$$H = SH_DS^{-1},$$

= SH_DS , (9)

where S is an orthogonal matrix, $S\tilde{S} = 1$, and H_D is the diagonalized H, a small neighborhood dH of H is related to a small neighborhood dS of S via the commutator connection

$$dH = [dS\tilde{S}, H], \tag{10}$$

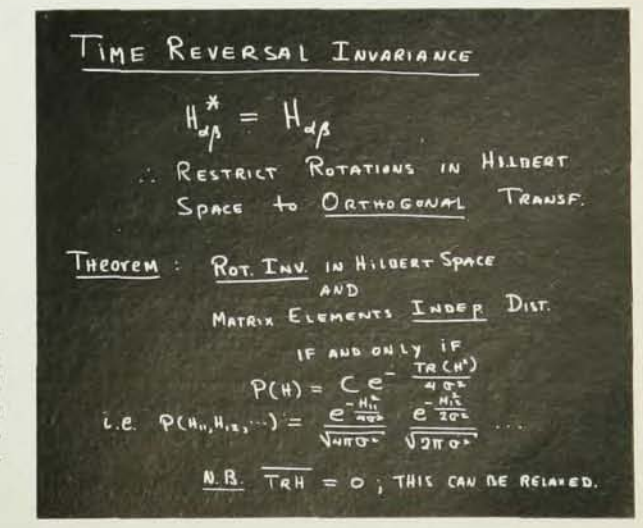


Fig. 19. Summary of underlying theory for the form-invariant, independent model of the fluctuations. This model (Gaussian ensemble) when fed into scheme of Fig. 4 leads to spacing, width, and expectation-value distributions.



The above experiment is associated with a program to develop radiation cooled components for use in high energy electron beam handling equipment. The apparatus shown is a mock up of a system which utilizes photoconductive cells to measure the temperature of a wheel rotating in a vacuum.

The engineer is testing a calibrating light source which will enable the performance of a photoconductive cell to be monitored periodically from a control console located a considerable distance from equipment subject to extremely intense ionizing radiation.

This experiment is just one of the many challenging problems under investigation at High Voltage Engineering Corporation. Engineers and Scientists are invited to investigate career opportunities.

> **Control Systems** Pulse Circuitry Stabilization Systems Magnetic Field Measuring Devices Magnet Optics

Please contact Mr. Louis A. Ennis P.O. Box 98 Burlington, Mass.



HIGH VOLTAGE ENGINEERING CORP.

BURLINGTON, MASSACHUSETTS (12 Miles North of Boston)

An equal opportunity employer

so that the parameterization of H is given in terms of the parameterization of S(N(N-1)/2) parameters), and the N eigenvalues of H make up the total of N(N+1)/2 parameters. This is the sort of measure introduced in the Gaussian ensemble. Rosenzweig's measure is, as has been stated, different, but involves the Hamiltonian directly and yields the same distributions for high-dimensional matrices.

In any event, since analytic work is so difficult, a continuing resort to Monte-Carlo machine computations can be foreseen to explore different models for the fluctuations. Especially, it may prove to be interesting to relax the plus-minus symmetry of the input matrix-element distributions and/or also their independent character.

The entire problem of fusing the various fluctuation ensembles with the usual statistical-mechanical functions, energy, entropy, specific heat, etc., in order to explore classes of systems as now permitted by the "new" statistical mechanics, remains wide open for effort. It is in this area that these various ensembles may prove to be extremely useful in order to gain insight into general properties of matter that do not seem to depend strongly on the details of the force laws but only on some rather general (one hopes "statistical") features of the laws. Not only will the usual point of view of statistical thermostatics be recast, but also statistical thermodynamics (the province of the Boltzmann equation and of the Pauli master equation) will probably feel the impact of the ensembles we have discussed. Again, because of the analytical difficulty, machine computations should be very helpful as a guide to the more fruitful directions for investigation.

References

T. Ericson, Phil, Mag. Suppl. 9, 425 (1960).
 Th. A. M. van Kleef, Proc. K. Ned. Akad. Wetensch. 63, 501-548 (1960).

- Campbell, Feshbach, Porter, and Weisskopf, Technical Report No. 73 Massachusetts Institute of Technology Laboratory for Nuclear Science and Engineering, Feb. 8, 1960 (unpublished).
- Chase, Wilets, and Edmonds, Phys. Rev. 110, 1080 (1958) 5. T. K. Kreuger and B. Margolis, Nuc. Phys. 28, 578 (1962). 6. F. Perey and B. Buck, Nuc. Phys. 32, 353 (1962)
- J. A. Harvey and D. J. Hughes, Phys. Rev. 109, 471 (1958).
- 8. Chrien, Bolotin, and Palevsky, Phys. Rev. (in press 9. M. Namiki, Prog. Theor. Phys. (Japan) 22, 843 (1959); 23, 629
- 10. Work carried out in collaboration with M. Goldberg.
- J. H. D. Jensen and J. M. Luttinger, Phys. Rev. 86, 907 (1952).
 M. L. Mehta, Nuc. Phys. 18, 395 (1960); M. L. Mehta and M. Gaudin, Nuc. Phys. 18, 420 (1960); 22, 340 (1960); M. Gaudin Nuc. Phys. 25, 447 (1960).
- 13. F. J. Dyson, J. Math. Phys. 3, 140-175 (1962).
- 14. N. Rosenzweig, Bull. Am. Phys. Soc. 7, 91 (1962). Charlotte E. Moore, Atomic Energy Levels; NBS Circular 467, Washington, D. C.; Vol. I., June 15, 1949; Vol. II., Aug. 15, 1952, Vol. III., May 1, 1958.
- C. E. Porter, Bull. Am. Phys. Soc. 29, 25 (1954).
- A. A. Abrahamson, Phys. Rev. 123, 538 (1961).
 C. H. Corliss and W. R. Bozman, Experimental Transition Probabilities for Spectral Lines of Seventy Elements; National Bureau of Standards Monograph 53, Washington, D. C.; July 20, 1962.